

---

# Understanding Adversarial Transferability in Federated Learning

---

Yijiang Li<sup>1†</sup> Ying Gao<sup>2</sup> HaoHan Wang

<sup>1</sup>Johns Hopkins University <sup>3</sup>South China University of Technology

<sup>4</sup>University of Illinois Urbana-Champaign

<sup>1</sup>yli556@jhu.edu, <sup>3</sup>haohanw@illinois.edu

## Abstract

We investigate the robustness and security issues from a novel and practical setting: a group of malicious clients has impacted the model during training by disguising their identities and acting as benign clients, and only revealing their adversary position after the training to conduct transferable adversarial attacks with their data, which is usually a subset of the data that FL system is trained with. Our aim is to offer a full understanding of the challenges the FL system faces in this practical setting across a spectrum of configurations. We notice that such an attack is possible, but the federated model is more robust compared with its centralized counterpart when the accuracy on clean images is comparable. Through our study, we hypothesized the robustness is from two factors: the decentralized training on distributed data and the averaging operation. We provide evidence from both the perspective of empirical experiments and theoretical analysis. Our work has implications for understanding the robustness of federated learning systems and poses a practical question for federated learning applications.

## 1 Introduction

The proliferation of mobile devices leads to a surge in user-end data collection. If utilized effectively, this sensitive data can enhance intelligent systems. Federated Learning (FL) offers a decentralized learning solution, training models via local updates and parameter aggregation [30]. The FL system, comprising a federation of clients and a data-less centralized server, circulates the global model amongst a random subset of participants. Participants perform local updates and submit them to the server for aggregation. The system’s design leverages private data while preserving privacy.

Although FL safeguards privacy, it is still susceptible to attacks such as data poisoning [22], model poisoning [3, 2], free-riders attack [27], and reconstruction attacks [15, 50]. It is also vulnerable to adversarial attacks during inference [4, 37], including adversarial examples designed to deceive the model [51]. Research on robust FL methods against adversarial examples has primarily focused on a white-box setting where attackers have full model access [49, 33, 21]. However, real-world FL applications, like Gboard [19], usually restrict such access.

We observe a distinct FL security challenge: malicious clients may pose as benign contributors, only revealing their adversarial intent post-training. These clients gain access to a subset of the training data, enabling potential adversarial attacks. Current FL applications lack effective mechanisms to eliminate such hostile participants [19], even if selection mechanisms exist, such as Krum [13, 25, 2], as attackers do not exhibit hostile behavior during training. After obtaining data, an attacker could train a substitute model for transfer-based black-box attacks.

In this paper, we pioneer an exploration of this practical perspective of FL robustness. Stemming from the above scenarios, we propose a simple yet practical assumption: the attacker possesses a limited amount of the users’ data but no knowledge about the target model or the full training set. To assess current FL system robustness and guide future research in this regard, we investigate the adversarial transferability under a spectrum of practical FL settings.

Preprint. Under review.

We first evaluate the transferability of adversarial examples generated from different source models to attack a federated-trained model. Then a comprehensive evaluation of practical configurations is conducted to assess the feasibility of our attack. We further investigate two properties of FL, namely the decentralized training and the averaging operation, and their correlation with federated robustness. To provide a comprehensive evaluation in a practical aspect, we take into account the attack timing, the architecture and different aggregation methods in our experiments. We have the following findings:

- We find that, while there are indeed security challenges from the novel attack setting, the federated model is more robust under white-box attack compared with its centralized-trained counterpart when their accuracy on clean images is comparable.
- We investigate the transferability of adversarial examples generated from models trained by various number of users' data. We observe that without any elaborated techniques such as dataset synthesis [32] or attention [42], a regularly trained source model with only limited users' data can perform the transfer attack. With ResNet50 on CIFAR10, we achieve a transfer rate of 70% and 80% with only 5% and 7% of users with augmentations and further improve this number to 81% and 85% with auto attack [9].
- We investigate two intrinsic properties of the FL, namely the property of distributed training and the averaging operation and discover that both heterogeneity and dispersion degree of the decentralized data as well as the averaging operations can significantly decrease the transfer rate of transfer-based black-box attack.
- To further understand the phenomenon, We provide theoretical analysis to further explain the observations.

## 2 Background

### 2.1 Adversarial Robustness

The adversarial robustness of a model is usually defined as the model's ability to predict consistently in the presence of small changes in the input. Intuitively, if the changes to the image are so tiny that they are imperceptible to humans, these perturbation will not alter the prediction. Formally, given a well trained classifier  $f$  and image-label pairs  $(x, y)$  on which the model correctly classifies  $f(x) = y$ ,  $f$  is defined to be  $\epsilon$ -robust with respect to distance metric  $d(\cdot; \cdot)$  if

$$\mathbb{E}_{(x,y)} \min_{x':d(x',x)\leq\epsilon} \alpha(f(x';\theta), y) = \mathbb{E}_{(x,y)} \alpha(f(x;\theta), y) \quad (1)$$

which is usually optimized through maximizing:

$$\mathbb{E}_{(x,y)} \min_{x':d(x',x)\leq\epsilon} \alpha(f(x';\theta), y) \quad (2)$$

where  $\alpha$  denotes the function evaluating prediction accuracy. In the case of classification,  $\alpha(f(x; \theta), y)$  yields 1 if the prediction  $f(x; \theta)$  equals ground-truth label  $y$ , 0 otherwise. The distance metric  $d(\cdot; \cdot)$  is usually approximated by  $L_0$ ,  $L_2$  or  $L_\infty$  to measure the visual dissimilarity of original image  $x$  and the perturbed image  $x'$ . Despite the change to the input is small, the community have found a class of methods that can easily manipulate model's predictions by introducing visually imperceptible perturbations in images [37, 17, 31]. From the optimization standpoint, it is achieved by maximizing the loss of the model on the input [29]:

$$\max_{\delta} l(f(x + \delta; \theta), y) \text{ s.t. } d(x + \delta, x) < \epsilon \quad (3)$$

where  $l(\cdot, \cdot)$  denotes the loss function (e.g. cross entropy loss) for training the model  $f$  parameterized by  $\theta$ . While these attack methods are powerful, they usually require some degrees of knowledge about the target model  $f$  (e.g. the gradient). Arguably, for many real-world settings, such knowledge is not available, and we can only expect less availability of such knowledge on FL applications trained and deployed by service providers. On the other hand, the hostile attacker having access to some but limited amount of users' data is a much more realistic scenario. Thus, we propose the following assumption for practical attack in FL: given the data of  $n$  malicious users  $D_m = \bigcup_{i=1}^n D_i$  where  $D_i = \{(x_k, y_k) | k = 1, \dots, m_i\}^{(i)}$  contains  $m_i$  data points, we aim to acquire a transferable perturbation  $\delta$  by maximizing the same objective as in Equation 3 but with a substitute model  $f'$  parameterized by  $\theta'$  trained by  $D_m$ :

$$\delta = \arg \min_{\delta} l(f'(x + \delta; \theta'), y) \text{ s.t. } d(x + \delta, x) < \epsilon \quad (4)$$

We hope to test whether this  $\delta$  can be used to deceive the target model  $f$  as well.

## 2.2 The Security and Robustness of Federated Learning

**Poisoning and Backdoor Attack.** Poisoning attacks [5, 13] aim to disrupt the global model by injecting malicious data or manipulating local model parameters on compromised devices. In contrast, backdoor attacks [2, 36] infuse a malicious task into the existing model without impacting its primary task accuracy, including model replacement [8], label-flipping [14], and the use of GANs [43]. Others have effectively incorporated weight boosting and stealth into the adversarial objective [3]. Defenses against these attacks often involve anomaly detection methods, such as Byzantine-tolerant aggregation [34] (e.g., Krum, MultiKrum [6], Bulyan [18], Trimmed-mean and Median [44]), focusing on the geometric distance between hostile and benign gradients. Additional strategies include clustering [35], Error Rate and Loss based Rejection [13], and learning a separate model to detect malicious updates [25, 24]. The robustness and attack performance of backdoor attacks is significantly influenced by FL data heterogeneity [46].

**Transfer Attack.** Transfer-based adversarial attacks employ the full training set of the target model to train a substitute model [48], a challenging condition to meet in practice, especially in FL where data privacy is paramount. Another line of inquiry delves into the mechanisms of black-box attacks, which exploit the high transferability of adversarial examples even between different model architectures [37, 17]. This transferability is partially attributed to the similarity between source and target models [17, 28], as adversarial perturbations align closely with a model’s weight vectors, and different models learn similar decision boundaries for the same task. [38] found that adversarial examples span a large, contiguous subspace, facilitating transferability. Meanwhile, [23] posits that adversarial perturbations are non-robust features captured by the model, and [40] utilizes this theory to explain differing mistakes in transfer attacks. Additionally, [12] reveals that similar gradients in source and target models and lower variance in loss landscapes increase transfer attack probability. We underscore our setting’s distinctiveness and importance compared to others.

**Key Difference 1:** Different from query-based or transfer-based black-box attack, we assume the malicious clients possess the data themselves, impacting the target model during training and attack during inference. We also present a comparison of our attack setting and the query-based attack in Appendix A. Note that our attack setting doesn’t contradict with the query-based attack. In fact, we can perform with both if the FL system allows a certain number of queries, which we leave to future works to explore.

**Key Difference 2:** Poisoning attack or backdoor attack manipulates the parameters update during target model training which can be defended by anomaly detection. Moreover, in practice, despite clients preserving the training data locally, the training procedure and communication with the server are highly encapsulated and encrypted with secret keys, which is even more unrealistic and laborious to manipulate. Our attack setting circumvents this risk since no hostile action is performed during the training but successfully boost the attack possibility during inference time.

**Significance:** Besides the potential data leakage by malicious participants, we also emphasize that despite, ideally, each participant having access to the global model, in real-world applications (e.g. Gboard [19]), the infrastructure provider will impose additional protection such as encryption or encapsulation over the local training. For instance, Gboard from Google provides the next-word prediction with FL, which requires users to install an app to participate. For an adversary, it’s impractical to obtain the global model without breaking or hacking the app or hijacking and decrypting the communication, despite all the things happening "locally". We believe this is much more difficult and laborious than our setting which significantly boosts the transferability by simply acting as a benign.

## 3 Investigation Setup and Research Goals

With the possibility that malicious client disguise to be a benign during training and exploit the obtained data for adversarial attacks, as discussed in Section 1, it is of necessity to investigate the robustness of federated model against transfer-based attack, *i.e.* transferability of adversarial examples against FL. More importantly, we want to understand where do the robustness of FL comes from and how the core components of FL effects it. To this end, we put forward the following research goals:

**GOAL 1:** We aim to investigate the possibility of a transfer attack with limited data and validate whether it is possible and practical for the attacker to lay benign during the training process and leverage the obtained data to perform the adversarial attack.

**GOAL 2:** We aim to explore how different degrees of decentralization, the heterogeneity of data and the aggregation, *i.e.* average affect the transferability of the adversarial examples against the FL model in a practical configuration.

### 3.1 Experiment Setup

**Threat Model.** Following [51], we use PGD [29] with 10 iterations, no random restart, and an epsilon of  $8 / 255$  over  $L_\infty$  norm on CIFAR10.

**Settings.** We first build up the basic FL setting. We split the dataset into 100 partitions of equal size in an iid fashion. We adopt two models for the experiments: CNN from [30] since it is commonly used in the FL literature and the widely used ResNet50[20] which represents a more realistic evaluation. We conduct training in three paradigms: the centralized model, federated model and the source model with limited number of clients’ data. For federated model, we use SGD without momentum, weight decay of  $1e-3$ , learning rate of 0.1, local batch size of 50 following [1]. We train locally 5 epochs on ResNet50 and 1 epoch on CNN. For centralized and source model training, we leverage SDG with momentum of 0.9, weight decay of  $1e-3$ , learning rate of 0.01 and batch size of 64. For adversarial training, we use the same setting as centralized and leverage PGD to perform the adversarial training. We refer to [51] for the detail of adversarial training. All experiments are conducted with one RTX 2080Ti GPU.

**Metrics.** We report Accuracy (Acc) and adversarial accuracy (Adv.Acc) for the performance and the robustness white-box attack, and for adversarial transferability, we report transfer accuracy (T.Acc) and transfer success rate (T.Rate) as detailed in 3.2.

### 3.2 Adversarial Transferability in Federated Learning

To define the transferability of adversarial examples, we first introduce the definition of the source model, target model and adversarial example. The source model is the substitute model used to generate adversarial examples while the target model is the target aimed to attack. Given the validation set  $x = \{(x_i, y_i)\}$ , source model  $f'$ , target model  $f$  and adversarial perturbation function  $adv(\cdot, \cdot)$  (e.g. PGD), we first define the following sets:  $s1 = \{x_i | f'(x_i) = y_i\}$ ,  $s2 = \{x_i | f'(adv(x_i, f')) \neq y_i\}$ ,  $s3 = \{x_i | f(x_i) = y_i\}$ ,  $s4 = \{x_i | f(adv(x_i, f')) \neq y_i\}$ . Adversarial examples are defined to be those samples that are originally correctly classified by model  $f'$  but are mis-classified when adversarial perturbation is added, *i.e.*,  $s1 \cap s2$ . Adversarial transferability against the target model refers to the ability of an adversarial examples generated from the source model to attack the target model (becomes an adversarial example of target model). We define transfer rate (T.Rate) and transfer accuracy (T.Acc) to measure the adversarial transferability:

$$\text{T.Rate} = \frac{||s1 \cap s2 \cap s3 \cap s4||}{||s1 \cap s2 \cap s3||}, \quad \text{T.Acc} = 1 - \frac{||s4||}{||x||} \quad (5)$$

where  $|| \cdot ||$  denotes the cardinality of a set.

### 3.3 Robustness with Comparable Accuracy

We first provide a preliminary understanding about the robustness of FL model. We train centralized model for 200 epochs and federated model for 400 rounds resulting in a decent accuracy of over 90% (see the regular column of Table 1). For CNN model, we train 200 epochs for centralized model and 600 rounds for federated model to achieve and accuracy of over 75%. We can observe that both clean and adversarial accuracy of federated model is lower than its centralized counterpart, aligned as the result in [51]. However, we conjecture that such an increase in adversarial accuracy is not attributed to the intrinsic robustness of centralized model but largely due to its high clean accuracy. To validate this hypothesis and facilitate a fair comparison between the two paradigms, we early-stop both models when their clean accuracy reach 90% (75% for CNN) and report the results in the same-acc column of Table 1. We early stop at 80% for adversarial training (72% for CNN). We can see, when both models reach a comparable

Table 1: Centralized and federated model under white-box attack.

Paradigm	Architecture	same-acc		regular	
		Acc	Adv.A	Acc	Adv.A
centralized	R50	90.20	0.01	95.24	0.40
	R50 (adv)	81.23	23.27	89.46	46.09
	CNN	75.06	1.24	82.41	0.35
	CNN (adv)	73.15	20.89	76.78	28.92
federated	R50	90.29	0.05	92.31	0.02
	R50 (adv)	80.05	36.44	81.05	39.11
	CNN	75.09	3.68	76.83	3.98
	CNN (adv)	72.85	25.5	72.87	24.35

clean accuracy, federated model shows greater robustness against white-box attack compared with the centralized model.

## 4 Experiments

After having some preliminary understandings regarding the robustness of FL under white-box attack, we discuss the transfer attack with limited data in this section. As described in Section 1, a much more realistic setting is that a group of hostile clients lay benign during training and leverage the fraction of training data to perform transfer attack. Consequently, the robustness against transfer attack of the FL model becomes vital in evaluating the security and robustness of FL applications. In this section, we first discuss the transfer attack in Section 4.1 and then explore the possibility of attacking with limited data in Section 4.2.

### 4.1 Robustness Against Transfer Attack

We explore the examples generated by two different training paradigms and their transferability when applying them to different models. Since similarity of decision boundary and clean accuracy influences and reflects the transferability between models [17, 28, 12], we early stop both federated and centralized models at 90% of accuracy (75% for CNN). Note that we follow this training setting for the rest of this paper. From Table 2, we can see that the adversarial examples generated by federated model are **highly transferable** to both federated and centralized model while adversarial examples generated by centralized model exhibit less transferability. The T.Rate of federated-to-centralized attack is even larger than centralized-to-centralized attack. Secondly, T.Rate of adversarial examples between models trained under same paradigms is larger than models trained under different paradigms, which can be attributed to the difference of the two training paradigms, *e.g.* the discrepancy in the decision boundary [17, 28] or different sub-space [38].

Table 2: T.Rate and transfer accuracy of PGD attack between pairs of models using various training paradigms. The row and column denote the source and target model respectively. For each cell, the left is the transfer accuracy and the right is the T.Rate.

		federated	centralized
R50	federated	0.15 / 99.83	2.01 / 97.67
	centralized	24.28 / 71.94	7.41 / 91.48
CNN	federated	19.31 / 76.32	21.59 / 71.84
	centralized	30.57 / 56.59	22.62 / 68.19

### 4.2 Transfer Attack with limited data

In this section, we will evaluate the possibility of our proposed attack setting, *i.e.* transfer attack with limited data. To simulate this scenario, we fixed the generated partition used in the federated training and randomly selects a specified number of users as malicious clients whose data is available for performing the attack. To perform the transfer attack, we trains a substitute model in a centralized manner with the collected data. Training details are specified in Section 3.1. One of the key differences of proposed setting and conventional transfer-based attack is number of available data to train the substitute (source) model. The number of clients used to train the source model also serves as a key factor for a successful attack since one would reason that more data will lead to higher success rate. To provide an overview of the transferability of adversarial examples generated by the source model trained with different number of clients, we plot the their relation in Figure 1. We have the following observations:

- **Observation 1.** T.Rate increases as the number of users increases, which is consistently observed in both centralized and federated models.
- **Observation 2.** With only 20% of clients the source model achieves an T.Rate of 90% and 50% with ResNet50 and CNN respectively. We notice that with ResNet50, the T.Rate of 20% clients is even larger than a transfer attack with full training data (71.94% T.Rate). With CNN, the source model trained with 20% clients can achieve 50% T.Rate which only lags behind the transfer attack by 6% (56.59%).

From observation 2, we can see that the proposed attack can achieve comparable or even better T.Rate or lower T.Acc. Consequently, we can conclude that the proposed attack setting with limited data is likely to cause significant security breaches in the current and future FL applications. To further explain observation 1 and an intriguing phenomenon that the T.Rate of ResNet50 model rises to the peak and then decreases, we hypothesize that when the number of clients used to train the source model is small, the clean accuracy of the source model is also low, leading to a large discrepancy in the decision boundary. Increasing the number of users used in the source model minimizes such

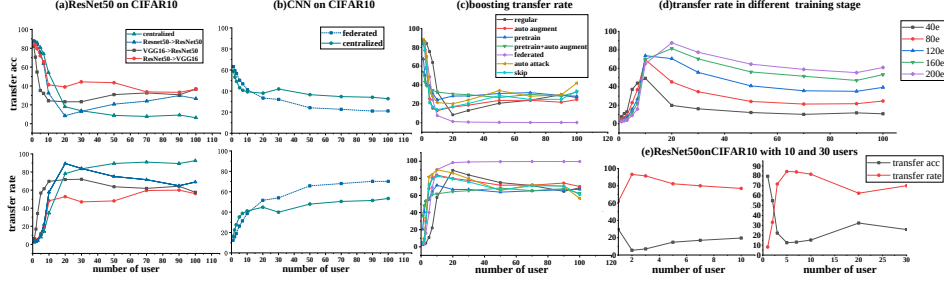


Figure 1: Attack with data from a limited number of users.

discrepancy until the amount of data is sufficient to train a source model with similar accuracy. At this point, the difference between the federated and centralized [7] becomes the dominant factor affecting the transferability since the source model is trained in centralized paradigm.

**Training substitute model in federated manner.** To testify the conjecture mentioned above, we train the substitute model with the same number of clients’ data in federated manner. Specifically, since we have the knowledge of each samples’ clients, we partition the collected data from malicious clients as the federated model trains the source model in federated manner. We discuss the importance of such knowledge to transfer attack in Appendix E. Results can be seen in (c) of Figure 1. We can see that, with federated source model, the T.Rate can be slightly boosted at the beginning (limited number of clients) but continue to increase as the number of users increases and finally contributes to a significantly high T.Rate of 99%. This demonstrates our conjecture regarding the trend and also shows that if the hostile party trains the substitute model in federated manner, the T.Rate can be further increased despite of its computation burden.

**Boosting transfer rate.** Following this conjecture, we first boost the T.Rate source model trained with limited data (*e.g.* 5 or 7 users) with data augmentation and model pretraining. Without loss of generality, in this paper, we leverage AutoAugment [10] and ImageNet pretrain. From (c) of Figure 1, we can clearly see, with these techniques we can successfully increase the T.Rate of 1% and 2% of clients from around 3% to 36% and 48% respectively. With 7% or 10% of clients’ data, the proposed attack setting achieves a high T.Rate of more than 80% (10% higher than the transfer-based attack). That is to say, with simple training techniques, malicious clients can attack with more than 40% of success rate with one or clients and 80% with 7 to 10 clients. To further illustrate the threat posed by our attack, we leverage the more advanced attack to replace the default PGD attack as shown in (c) of Figure 1. We can see that both auto-attack [9] and skip attack [41] achieve a transfer rate of over 80% with only 3 and 10 users respectively. Noticeably, auto-attack achieves the highest transfer rate of 85% with 10% of the users. These results further demonstrate the threat our attack poses.

**Practical evaluation.** To practically evaluate our attack setting, we consider two cases: 1. the malicious clients can only participate in some periods and 2. the attacker has no knowledge of the model deployed. We simulate these situations by attacking in different training stages and with different architectures, as shown in (d) of Figure 1 where a similar trend mentioned above is observed. We also conduct experiments with 10 and 30 users as shown in (e) of Figure 1 which we believe is a relatively simple setting that can further emphasize the threat of our attack setting.

## 5 Two intrinsic properties contributing to transfer robustness

To fully understand how adversarial examples transfer between centralized and federated models, we study two intrinsic properties of FL and its relation with transfer robustness. To protect the privacy of clients and leverage the massive data from user-end, FL utilizes distributed data to train a global model through local updates and aggregation at the server [30]. As a consequence, the distributed data and the aggregation operation is the core component of a FL method.

### 5.1 Decentralized training and data Heterogeneity

This section aims to explore the relationship between the degree of degree and transfer robustness.

**Control the degree of dispersion and heterogeneity.** To explore the impact of distributed data on adversarial transferability, we control decentralization and heterogeneity through four indexes. By varying the number of clients in the partition, we alter the degree of dispersion of distributed data. For heterogeneity, we change the number of maximum classes per client [30], the alpha value of

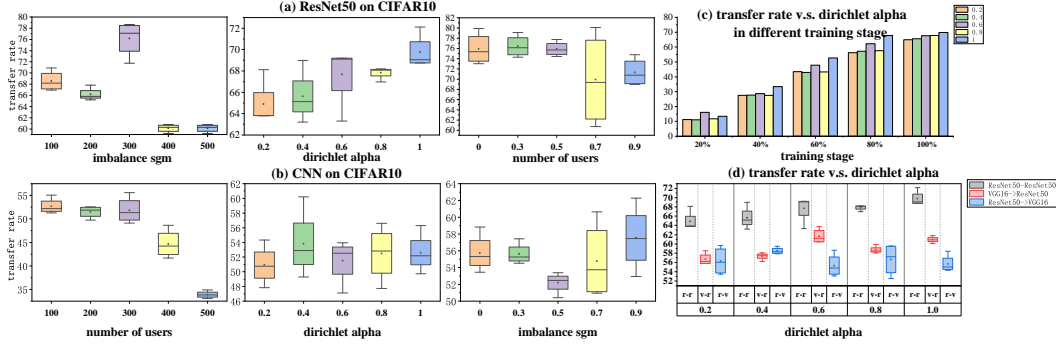


Figure 2: T.Rate vs. data of different heterogeneity and dispersion degree. (a): the top 3 are results of ResNet50; (b): the bottom 3 are results of CNN; Left: T.Rate as a function of the number of users in federated training; Middle: T.Rate as a function of dirichlet alpha; Right: T.Rate as a function of unbalanced sgm.

Dirichlet distributions ( $\alpha$ ) [39, 45] (smaller  $\alpha$  means a more non-iid partition) and the log-normal variance (sgm) of the Log-Normal distribution (larger variance denotes more unbalanced partitions) used in unbalanced partition [47]. We leverage FedLab framework to generate the different partitions [47]. For the rest experiments, we leverage the centralized trained model as the source to perform the transfer attack.

**Degree of decentralization reduces transferability.** As seen in Figure 2 (left of (a) and (b)), we can observe that T.Rate drops with an increasing number of users, which demonstrate that more decentralized data leads to lower transferability.

**Data heterogeneity affects transfer attack.** As per the middle plot of (a) and (b) in Figure 2, we can see that T.Rate increases clearly as  $\alpha$  increases. We report the results on different the number of maximum classes per client in Appendix B. We also explore whether unbalanced data leads to a decrease of transferability in Figure 2 (right of (a) and (b)), where larger variance leads to a lower transfer rate. To validate the above observation, we provide statistical testing for the correlation coefficient in Appendix C. With the Spearman correlation coefficient, we report a significant negative correlation on ResNet50 between log-normal variance and T.Rate under a significance level of 0.1 ( $p$ -value=0.05). We report a significant correlation on all results with a level of 0.05 except the CNN experiments with different Dirichlet  $\alpha$  and unbalanced sgm. We also visualize the linear regression results in Appendix I. Practically, we also evaluate this relation with more realistic attack settings. By attacking in different training stages and with different architectures as shown in (c) and (d) of Figure 2, we demonstrate that this correlation holds in various configurations. To sum up, we demonstrate that decentralized training reduces the transferability of adversarial examples. This can be attributed to the enlarged discrepancy of decision boundary between the source model and target model when the training data is more decentralized or heterogeneous. The heterogeneous distribution leads to a loss landscape significantly different from the ones of iid and centralized model and also results in a loss landscape with high variance [7], which all contribute to lower the transfer possibility of adversarial examples [12].

## 5.2 Averaging Leads to Robustness

We explore the other core property, averaging operation, of FL and its correlation with transfer robustness. To change the degree of averaging in FL, we modify the number of clients selected to average at each round. We use the centralized model and source model with 30 clients' data as substitute models to perform the transfer attack. Both models are early stopped at 90% as mentioned in Section 3.1. We train our federated target model with 100 users following Section 3.1. We plot the relation of T.Rate and the number of users in (a) to (d) of Figure 3. Both CNN and ResNet50 exhibit a decreasing trend as the number of clients used to average increases. We also provide statistical testing to validate the correlation in Appendix C. With the Spearman correlation coefficient, we report a significant negative correlation in all four experiments (all  $p$ -values are less than .001). To further validate this observation in more practical evaluations, we perform the attack in different training stages, with different architectures and different aggregation methods, as shown in (e), (f) of Figure 3 and Figure 6 in Appendix D, where similar trends can be observed. This evidence demonstrates that averaging in FedAvg improves the robustness of the federated model against transfer attacks.

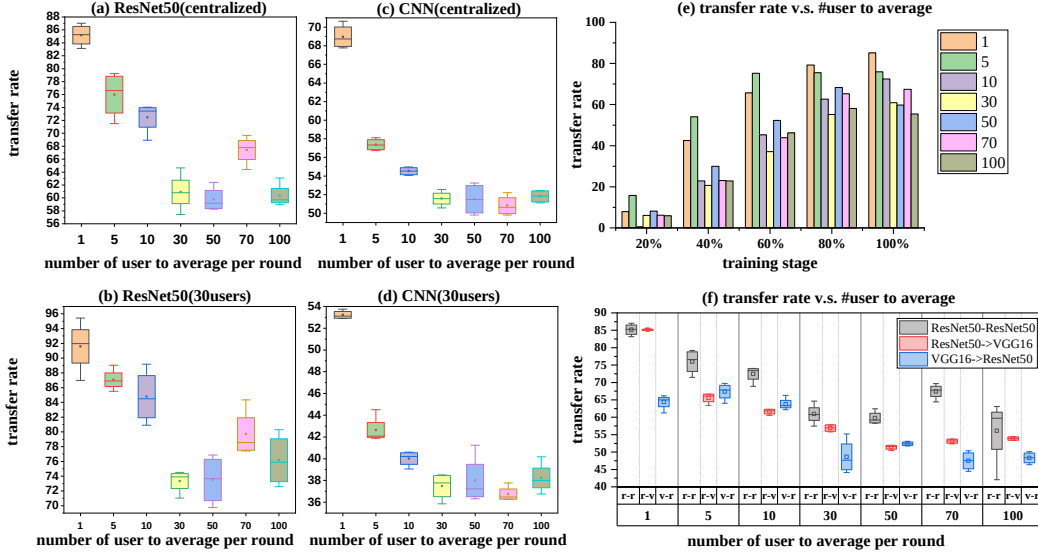


Figure 3: Transfer rate v.s. different number of clients selected to average in each round; (a) ResNet50 results with source model trained in centralized manner with full data; (b) ResNet50 results with source model trained with 30 users; (c) CNN results with source model trained in centralized manner with full data; (d) CNN results with source model trained with 30 users;

### 5.3 Discussion

We list the results of our investigations as the below take-home messages and their implications:

- The heterogeneous data and large degree of decentralization both result in lower transferability of adversarial examples from the substitute model. → The attacker can benefit from closing the discrepancy of substitute model and target model (*e.g.* train substitute model also in federated manner) in terms of transferring.
- With more clients to average at each round, the federated model becomes increasingly robust to black-box attack. → Defenders can benefit from increasing the number of clients selected at each round to average.
- In addition, we also identify a different, simpler, but practical attack evaluation for FL, which can serve as the standard robustness evaluation for future FL applications.

## 6 Theoretical Evidence

**Background.** We first introduce background and notation. We use  $(X, Y)$  to denote a dataset, where  $X \in \mathbb{R}^{n \times p}$  and  $Y \in \mathbb{R}^n$ . We use  $(x, y)$  to denote a sample following Section 2. We consider the problem of federated learning optimization model:

$$\min_{\theta} \{l(\theta) \triangleq \sum_{k=1}^N p_k l_k(\theta)\}, \quad \text{where} \quad l_k(\theta) = \frac{1}{n_k} \sum_{j=1}^{n_k} l(f(x; \theta), y) \quad (6)$$

$N$  is the total number devices and  $n_k$  is the number of samples possessed by device  $k$ .  $p_k$  is the weight of device  $k$  with the constraint that  $\sum p_k = 1$ . Following [26], we assume the algorithm performs a total of  $T$  stochastic gradient descent (SGD) iterations and each round of local training possesses  $E$  iterations.  $\frac{T}{E}$  is thus the total communication times. At each communication, a maximal number of  $K$  devices will participate in the process. We quantify the degree of non-iid using  $\Gamma = l_{\star} - \sum_{k=1}^N p_k l_{k\star}$  where  $l_{\star}$  and  $l_{k\star}$  is the minimum value of  $l(\theta)$  and  $l_k(\theta)$  respectively. We use the relative increase of adversarial loss [11] to measure the transferability for easier derivation:

$$R(x, y, \theta, \theta') = \frac{\nabla_x l(f'(x; \theta'), y)^T \nabla_x l(f(x; \theta), y)}{\|\nabla_x l(f'(x; \theta'), y)\|_2 \|\nabla_x l(f(x; \theta), y)\|_2} \quad (7)$$

We provide detail derivation in Appendix F. Following assumptions from [26], which we detail about in Appendix G, and additional assumptions for adversarial transferability, we provides a low bound for  $R$ .



**Assumption 1:**  $\partial f(x; \theta)/\partial x = \theta^T \rho(x, \theta)$  where  $\rho(x, \theta)$  is an arbitrary function in the forms of  $\rho(x, \theta) : \mathbb{R}^{1 \times p} \times \mathbb{R}^{p \times 1} \rightarrow \mathbb{R}$ .

There are many functions following our standards (e.g.  $\ell_2$ -norm regularized linear regression, logistic regression and softmax classifier). For the rest of our discussion, we define  $\nabla l(f(x; \theta), y) = \partial f(x; \theta)/\partial x$

**Lemma 6.1.** *With Assumption 1, we have*

$$R(x, y, \theta, \theta') = \frac{\theta^T \theta'}{\|\theta\|_2 \|\theta'\|_2} \leq 1 \quad (8)$$

With Lemma 6.1,  $\theta$  can be directly measured by the cosine similarity of the parameters  $\theta$  and  $\theta'$ . Furthermore, as we need to offer a discussion regarding multiple aspects of the model, such as the loss, the parameters, and the data, we follow the previous convention [26] to focus on a narrower scope the model family:

**Assumption 2:** Model  $f$  is in the form of  $f(\theta) = \sum_{x \in X} (x\theta)^2$ .

Notice that this is not a significant deviation from previous studies [26] that focus on  $f(\theta) = \theta^T A \theta$  for detailed investigation of the parameter behaviors.

**Assumption 3:** The covariance of the samples we study is positive semidefinite, i.e.,  $X^T X \succcurlyeq \mathbf{I}$

The following theorem also depends on assumptions made by [26] which is detailed in Appendix G (Assumption 4-8)

**Theorem 6.2.** *With Assumptions 2-8, we have:*

$$\mathbb{E}[R(x, y, \theta_*, \theta')] \geq \frac{2\mu(\gamma + T - 1)\theta_*^T \theta_*}{4(B + C)\kappa + \mu^2\gamma\kappa\mathbb{E}\|\theta_1 - \theta_*\|^2} \quad (9)$$

where  $L, \mu, \sigma_k, G$  are defined in the assumptions,  $\kappa = \frac{L}{\mu}$ ,  $\gamma = \max\{8\kappa, E\}$ ,  $B = \sum_{k=1}^N p_k^2 \sigma_k^2 + 6L\Gamma + 8(E - 1)^2 G^2$  and  $C = \frac{4}{K} E^2 G^2$ .  $\theta_1$  is the parameter after one step update of SGD.  $\theta_*$  is the optimal parameter for centralized model.

**Corollary 6.3.** *With Theorem 6.2, we can derive the lower bound of the expectation of  $R(x, y, \theta_*, \theta'')$  by setting  $E = 1$  and  $K = 1$ , where  $\theta''$  represents the centralized source model.*

$$\mathbb{E}[R(x, y, \theta_*, \theta'')] \geq \frac{2\mu(\gamma + T - 1)\theta_*^T \theta_*}{4(\sum_{k=1}^N p_k^2 \sigma_k^2 + 6L\Gamma + 4G^2)\kappa + \mu^2\gamma\kappa\mathbb{E}\|\theta_1 - \theta_*\|^2} \quad (10)$$

**Remark 6.4.** The difference between the lower bound of FL (Lemma 6.1) and the centralized model (Corollary 6.3) lies in the denominator. With FL model,  $B + C = \sum_{k=1}^N p_k^2 \sigma_k^2 + 6L\Gamma + 8(E - 1)^2 G^2 + \frac{4}{K} E^2 G^2$ , while centralized gives a smaller  $B + C = \sum_{k=1}^N p_k^2 \sigma_k^2 + 6L\Gamma + 4G^2$ , which leads to a larger lower bound. Thus, the transferability of adversarial examples generated by the surrogate centralized model to attack the federated model is less than that when attacking a centralized model.

Remark 6.4 supports the empirical findings in Section 4.1.

**Remark 6.5.** With Theorem 6.2, we can see the degree of non-iid  $\Gamma$  lies in the denominator of the lower bound, meaning that the larger the degree of non-iid among devices, the less the transferability of examples generated by centralized surrogate model.

Remark 6.5 aligns with our empirical findings in Section 5.1, which will provide more insights to future research on federated adversarial robustness.

**Theorem 6.6.** *Let  $\mathcal{T}$  denote the train set  $\mathcal{T} = (X, Y)$  sampled from some data distribution and  $x'$  denote the adversarial example following some adversarial distribution. Let  $f(\cdot, \mathcal{T})$  be the model trained with dataset  $\mathcal{T}$  and  $f(\cdot) = \mathbb{E}_{\mathcal{T}}[f(\cdot; \mathcal{T})]$  is the expectation of the model trained on dataset  $\mathcal{T}$ . We denote the an average of  $n$  models as  $f_n = \frac{1}{n} \sum_{i=1}^n f_i(\cdot; \mathcal{T}_i)$ . Then we have:*

$$\mathbb{E}_{x', y} \mathbb{E}_{\mathcal{T}}[\|y - f_n(x')\|_2^2] = \mathbb{E}_{x', y}[\|y - \bar{f}(x')\|_2^2] + \frac{1}{n} \mathbb{E}_{x', \mathcal{T}}[\|\bar{f}(x') - f(x', \mathcal{T})\|_2^2] \quad (11)$$

**Remark 6.7.** In Theorem 6.6,  $\mathbb{E}_{x', y}[\|y - \bar{f}(x')\|_2^2]$  and  $\mathbb{E}_{x', \mathcal{T}}[\|\bar{f}(x') - f(x', \mathcal{T})\|_2^2]$  only depends on  $f$  and are fixed with respect to  $n$ . Thus, as  $n$  becomes larger, the expected error decreases.

Remark 6.7 supports the observation in Section Section 5.2.

## 7 Conclusion

This paper explores the potential for malicious clients to masquerade as benign entities in Federated Learning, then exploit this position to launch transferable attacks. Our evaluation shows that limited data can yield a comparable transfer rate to a full-dataset attack. We discover that decentralized training, heterogeneous data, and averaging operations enhance transfer robustness and reduce the transferability of adversarial examples.

**Ethics Statement** In this work, we aim to further understand the security challenges a Federated Learning system can face in reality with a new and practical settings. We believe our study will benefit the society with a full understanding of the working mechanism of the potential attacks in the scenario raised in the paper, and thus build the ground for continued study of the methods that are secure against such threats.

## References

- [1] Durmus Alp Emre Acar, Yue Zhao, Ramon Matas Navarro, Matthew Mattina, Paul N Whatmough, and Venkatesh Saligrama. Federated learning based on dynamic regularization. *arXiv preprint arXiv:2111.04263*, 2021.
- [2] Eugene Bagdasaryan, Andreas Veit, Yiqing Hua, Deborah Estrin, and Vitaly Shmatikov. How to backdoor federated learning. In *International Conference on Artificial Intelligence and Statistics*, pages 2938–2948. PMLR, 2020.
- [3] Arjun Nitin Bhagoji, Supriyo Chakraborty, Prateek Mittal, and Seraphin Calo. Analyzing federated learning through an adversarial lens. In *International Conference on Machine Learning*, pages 634–643. PMLR, 2019.
- [4] Battista Biggio, Iginio Corona, Davide Maiorca, Blaine Nelson, Nedim Šrđić, Pavel Laskov, Giorgio Giacinto, and Fabio Roli. Evasion attacks against machine learning at test time. In *Joint European conference on machine learning and knowledge discovery in databases*, pages 387–402. Springer, 2013.
- [5] Battista Biggio, Blaine Nelson, and Pavel Laskov. Poisoning attacks against support vector machines. *arXiv preprint arXiv:1206.6389*, 2012.
- [6] Peva Blanchard, El Mahdi El Mhamdi, Rachid Guerraoui, and Julien Stainer. Machine learning with adversaries: Byzantine tolerant gradient descent. *Advances in Neural Information Processing Systems*, 30, 2017.
- [7] Debora Caldarola, Barbara Caputo, and Marco Ciccone. Improving generalization in federated learning by seeking flat minima. *arXiv preprint arXiv:2203.11834*, 2022.
- [8] Xinyun Chen, Chang Liu, Bo Li, Kimberly Lu, and Dawn Song. Targeted backdoor attacks on deep learning systems using data poisoning. *arXiv preprint arXiv:1712.05526*, 2017.
- [9] Francesco Croce and Matthias Hein. Reliable evaluation of adversarial robustness with an ensemble of diverse parameter-free attacks. In *International conference on machine learning*, pages 2206–2216. PMLR, 2020.
- [10] Ekin D Cubuk, Barret Zoph, Dandelion Mane, Vijay Vasudevan, and Quoc V Le. Autoaugment: Learning augmentation policies from data. *arXiv preprint arXiv:1805.09501*, 2018.
- [11] Ambra Demontis, Marco Melis, Maura Pintor, Matthew Jagielski, B. Biggio, Alina Oprea, C. Nita-Rotaru, and F. Roli. Why do adversarial attacks transfer? explaining transferability of evasion and poisoning attacks. *Usenix Security Symposium*, 2018.
- [12] Ambra Demontis, Marco Melis, Maura Pintor, Matthew Jagielski, Battista Biggio, Alina Oprea, Cristina Nita-Rotaru, and Fabio Roli. Why do adversarial attacks transfer? explaining transferability of evasion and poisoning attacks. In *28th USENIX security symposium (USENIX security 19)*, pages 321–338, 2019.

- [13] Minghong Fang, Xiaoyu Cao, Jinyuan Jia, and Neil Gong. Local model poisoning attacks to {Byzantine-Robust} federated learning. In *29th USENIX Security Symposium (USENIX Security 20)*, pages 1605–1622, 2020.
- [14] Clement Fung, Chris JM Yoon, and Ivan Beschastnikh. Mitigating sybils in federated learning poisoning. *arXiv preprint arXiv:1808.04866*, 2018.
- [15] Jonas Geiping, Hartmut Bauermeister, Hannah Dröge, and Michael Moeller. Inverting gradients-how easy is it to break privacy in federated learning? *Advances in Neural Information Processing Systems*, 33:16937–16947, 2020.
- [16] Stuart Geman, Elie Bienenstock, and René Doursat. Neural networks and the bias/variance dilemma. *Neural computation*, 4(1):1–58, 1992.
- [17] Ian J Goodfellow, Jonathon Shlens, and Christian Szegedy. Explaining and harnessing adversarial examples. *arXiv preprint arXiv:1412.6572*, 2014.
- [18] Rachid Guerraoui, Sébastien Rouault, et al. The hidden vulnerability of distributed learning in byzantium. In *International Conference on Machine Learning*, pages 3521–3530. PMLR, 2018.
- [19] Andrew Hard, Kanishka Rao, Rajiv Mathews, Swaroop Ramaswamy, Françoise Beaufays, Sean Augenstein, Hubert Eichner, Chloé Kiddon, and Daniel Ramage. Federated learning for mobile keyboard prediction. *arXiv preprint arXiv:1811.03604*, 2018.
- [20] Kaiming He, Xiangyu Zhang, Shaoqing Ren, and Jian Sun. Deep residual learning for image recognition. In *Proceedings of the IEEE conference on computer vision and pattern recognition*, pages 770–778, 2016.
- [21] Junyuan Hong, Haotao Wang, Zhangyang Wang, and Jiayu Zhou. Federated robustness propagation: Sharing adversarial robustness in federated learning. *arXiv preprint arXiv:2106.10196*, 2021.
- [22] Ling Huang, Anthony D Joseph, Blaine Nelson, Benjamin IP Rubinstein, and J Doug Tygar. Adversarial machine learning. In *Proceedings of the 4th ACM workshop on Security and artificial intelligence*, pages 43–58, 2011.
- [23] Andrew Ilyas, Shibani Santurkar, Dimitris Tsipras, Logan Engstrom, Brandon Tran, and Aleksander Madry. Adversarial examples are not bugs, they are features. *Advances in neural information processing systems*, 32, 2019.
- [24] Tung Kieu, Bin Yang, Chenjuan Guo, and Christian S Jensen. Outlier detection for time series with recurrent autoencoder ensembles. In *IJCAI*, pages 2725–2732, 2019.
- [25] Suyi Li, Yong Cheng, Wei Wang, Yang Liu, and Tianjian Chen. Learning to detect malicious clients for robust federated learning. *arXiv preprint arXiv:2002.00211*, 2020.
- [26] Xiang Li, Kaixuan Huang, Wenhao Yang, Shusen Wang, and Zhihua Zhang. On the convergence of fedavg on non-iid data. In *8th International Conference on Learning Representations, ICLR 2020, Addis Ababa, Ethiopia, April 26-30, 2020*. OpenReview.net, 2020.
- [27] Jierui Lin, Min Du, and Jian Liu. Free-riders in federated learning: Attacks and defenses. *arXiv preprint arXiv:1911.12560*, 2019.
- [28] Yanpei Liu, Xinyun Chen, Chang Liu, and Dawn Song. Delving into transferable adversarial examples and black-box attacks. *arXiv preprint arXiv:1611.02770*, 2016.
- [29] Aleksander Madry, Aleksandar Makelov, Ludwig Schmidt, Dimitris Tsipras, and Adrian Vladu. Towards deep learning models resistant to adversarial attacks. *arXiv preprint arXiv:1706.06083*, 2017.
- [30] Brendan McMahan, Eider Moore, Daniel Ramage, Seth Hampson, and Blaise Aguera y Arcas. Communication-efficient learning of deep networks from decentralized data. In *Artificial intelligence and statistics*, pages 1273–1282. PMLR, 2017.

- [31] Seyed-Mohsen Moosavi-Dezfooli, Alhussein Fawzi, and Pascal Frossard. Deepfool: a simple and accurate method to fool deep neural networks. In *Proceedings of the IEEE conference on computer vision and pattern recognition*, pages 2574–2582, 2016.
- [32] Nicolas Papernot, Patrick McDaniel, Ian Goodfellow, Somesh Jha, Z Berkay Celik, and Ananthram Swami. Practical black-box attacks against machine learning. In *Proceedings of the 2017 ACM on Asia conference on computer and communications security*, pages 506–519, 2017.
- [33] Amirhossein Reisizadeh, Farzan Farnia, Ramtin Pedarsani, and Ali Jadbabaie. Robust federated learning: The case of affine distribution shifts. *Advances in Neural Information Processing Systems*, 33:21554–21565, 2020.
- [34] Virat Shejwalkar and Amir Houmansadr. Manipulating the byzantine: Optimizing model poisoning attacks and defenses for federated learning. In *NDSS*, 2021.
- [35] Shiqi Shen, Shruti Tople, and Prateek Saxena. Auror: Defending against poisoning attacks in collaborative deep learning systems. In *Proceedings of the 32nd Annual Conference on Computer Security Applications*, pages 508–519, 2016.
- [36] Ziteng Sun, Peter Kairouz, Ananda Theertha Suresh, and H Brendan McMahan. Can you really backdoor federated learning? *arXiv preprint arXiv:1911.07963*, 2019.
- [37] Christian Szegedy, Wojciech Zaremba, Ilya Sutskever, Joan Bruna, Dumitru Erhan, Ian Goodfellow, and Rob Fergus. Intriguing properties of neural networks. *arXiv preprint arXiv:1312.6199*, 2013.
- [38] Florian Tramèr, Nicolas Papernot, Ian Goodfellow, Dan Boneh, and Patrick McDaniel. The space of transferable adversarial examples. *arXiv preprint arXiv:1704.03453*, 2017.
- [39] Hongyi Wang, Mikhail Yurochkin, Yuekai Sun, Dimitris Papailiopoulos, and Yasaman Khazaeni. Federated learning with matched averaging. *arXiv preprint arXiv:2002.06440*, 2020.
- [40] Futa Waseda, Sosuke Nishikawa, Trung-Nghia Le, Huy H Nguyen, and Isao Echizen. Closer look at the transferability of adversarial examples: How they fool different models differently. *arXiv preprint arXiv:2112.14337*, 2021.
- [41] Dongxian Wu, Yisen Wang, Shu-Tao Xia, James Bailey, and Xingjun Ma. Skip connections matter: On the transferability of adversarial examples generated with resnets. *arXiv preprint arXiv:2002.05990*, 2020.
- [42] Weibin Wu, Yuxin Su, Xixian Chen, Shenglin Zhao, Irwin King, Michael R Lyu, and Yu-Wing Tai. Boosting the transferability of adversarial samples via attention. In *Proceedings of the IEEE/CVF Conference on Computer Vision and Pattern Recognition*, pages 1161–1170, 2020.
- [43] Chulin Xie, Keli Huang, Pin-Yu Chen, and Bo Li. Dba: Distributed backdoor attacks against federated learning. In *International Conference on Learning Representations*, 2019.
- [44] Dong Yin, Yudong Chen, Ramchandran Kannan, and Peter Bartlett. Byzantine-robust distributed learning: Towards optimal statistical rates. In *International Conference on Machine Learning*, pages 5650–5659. PMLR, 2018.
- [45] Mikhail Yurochkin, Mayank Agarwal, Soumya Ghosh, Kristjan Greenewald, Nghia Hoang, and Yasaman Khazaeni. Bayesian nonparametric federated learning of neural networks. In *International Conference on Machine Learning*, pages 7252–7261. PMLR, 2019.
- [46] Syed Zawad, Ahsan Ali, Pin-Yu Chen, Ali Anwar, Yi Zhou, Nathalie Baracaldo, Yuan Tian, and Feng Yan. Curse or redemption? how data heterogeneity affects the robustness of federated learning. In *Proceedings of the AAAI Conference on Artificial Intelligence*, volume 35, pages 10807–10814, 2021.
- [47] Dun Zeng, Siqi Liang, Xiangjing Hu, and Zenglin Xu. Fedlab: A flexible federated learning framework. *arXiv preprint arXiv:2107.11621*, 2021.

- [48] Wen Zhou, Xin Hou, Yongjun Chen, Mengyun Tang, Xiangqi Huang, Xiang Gan, and Yong Yang. Transferable adversarial perturbations. In *Proceedings of the European Conference on Computer Vision (ECCV)*, pages 452–467, 2018.
- [49] Yao Zhou, Jun Wu, Haixun Wang, and Jingrui He. Adversarial robustness through bias variance decomposition: A new perspective for federated learning. *arXiv preprint arXiv:2009.09026*, 2020.
- [50] Ligeng Zhu, Zhijian Liu, and Song Han. Deep leakage from gradients. *Advances in neural information processing systems*, 32, 2019.
- [51] Giulio Zizzo, Amrith Rawat, Mathieu Sinn, and Beat Buesser. Fat: Federated adversarial training. *arXiv preprint arXiv:2012.01791*, 2020.

## A Comparison with query-based attack

Query-based black-box attack aims to attack the target model with limited queries to the target model. Through these queries, the source model manage to optimize the decision boundary towards the target model. However, most APIs and FL-based systems requires charges to access the service or equips anomaly detection that detects multiple or malicious queries. In this section, we provide a comparison of our proposed attack setting and the query-based black-box attack. To conduct a fair comparison, we follow the experiment setting in Section 4.2. With data from a limited number of users, instead of using the ground-truth class labels to train the source model, we query the target model for the prediction and set the predicted label as ground-truth. Note that, to facilitate the queries for the data from one client, one will have to perform 500 (in 100 clients partition) requests to the target model. The comparison is shown in Figure 4. We can see from Figure 4 that query-based outperforms the our proposed attack setting by a slight margin when the number of clients used to train the source model is small and the transfer rate of query-based attack continues to increase after 20 users where our attack setting begins to decrease. This can be attributed to the queries which help the source model to learn a more similar decision boundary. Through this experiment, we can hypothesize that, with some limited number of queries, our attack setting can be further boosted since it can help the substitute model to learn a similar loss landscape and decision boundary as the ones of target model.

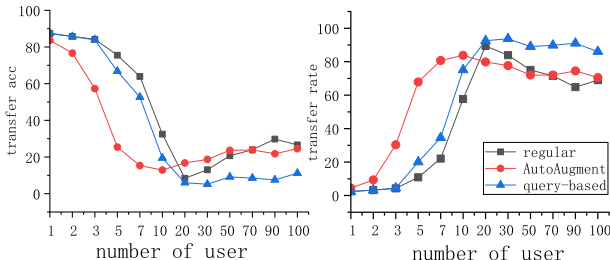


Figure 4: Comparison with query-based black-box attack; Left: transfer accuracy as a function of number of users' data leveraged in source model training; Right: transfer rate as a function of number of users' data leveraged in source model training;

## B Heterogeneity in pathological non-iid distribution

To prove generalization of our findings with other non-iid distribution, we follow [30] to generate pathological distribution (partition by shards). To partition CIFAR10 dataset into 100 clients, we first sort the samples by class label and then divide the data into  $n$  shards of size  $50000/n$  (e.g. 500 shards of size 100) and assign each client  $n/100$  shards. In this way, most client will have only samples of  $n/100$  classes [30]. By varying the number of shards  $n$ , we control the maximum number of classes in most clients and hence the degree of non-iid of partitions. We conduct experiments on two different settings, the 10 user partition and 100 user partition. For 10 user partition, we generate a partition comprised of 10 users and vary the number of shards  $n$  from 20 to 70. For 100 user partition, we generate a partition comprised of 100 users and vary the number of shards  $n$  from 200 to 700. We generate the transfer rate v.s. maximum number of classes plots as in the Section 5.1. We can observe from Figure 5 a increase trend in both experiment settings with ResNet50 and CNN which demonstrates that our findings hold under different ways of simulating data heterogeneity. We also perform hypothesis testing for this correlation in Appendix C. All four experiments show significant correlation under a level of 0.01.

Notice we also find that the transfer rate of 10 users experiment is consistently larger than the 100 users setting which further demonstrates our findings in Section 5.1 that more decentralized training leads to lower adversarial transferability for federated model.

## C Statistical Hypothesis Testing on Spearman correlation coefficient

We demonstrates the correlation between different degree of decentralization, heterogeneity of training data and transferability of adversarial examples in Section 5.1 through plots and graphs and

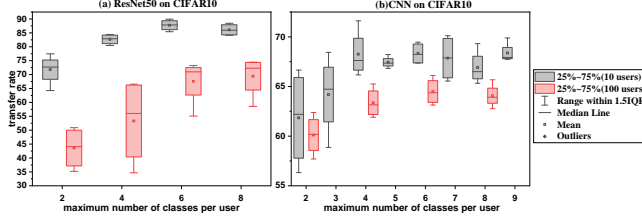


Figure 5: Transfer rate v.s. maximum number of classes per client; (a): Results of ResNet50 on CIFAR10 dataset; (b): Results of CNN on CIFAR10 dataset;

show that with more decentralized, heterogeneous data, the federated model is more robust to transfer attack. We also display a negative relation between the number of clients to average and transfer success rate through box charts in Section 5.2.

To statistically validate these correlations, we perform two-tailed Hypothesis Testing on Spearman correlation coefficient. To conduct Hypothesis Testing for Spearman correlation coefficient on a specified correlation, we first calculate the Spearman correlation coefficient  $\rho$  on the two sets of points (e.g. T.Rate and Dirichlet  $\alpha$ ):

$$\rho = \frac{\text{cov}(X, Y)}{\sigma(X)\sigma(Y)}$$

where  $\text{cov}(\cdot, \cdot)$  denotes the covariance and  $\sigma(\cdot)$  represents the standard deviation. To perform the Hypothesis Test, we first have the Null Hypothesis  $H_0$  and Alternate Hypothesis  $H_a$ :

$$H_0 : \rho = 0$$

$$H_a : \rho \neq 0$$

We choose the significance level to be 0.1, which means we reject  $H_0$  if p-value is smaller than 0.1. We report the p-value and Spearman correlation coefficient in Table 3.

Table 3: Spearman correlation coefficient and p-value

Architecture	X	p-value (two-tailed)	Spearman coefficient
ResNet50	dirichlet $\alpha$	.006	.59
	unbalance sgm	.05	-.44
	number of user in partition	.003	-.63
	maximum number of classes (10 users)	< .001	0.80
	maximum number of classes (100 users)	< .001	.76
	number of user to average (30 users)	< .001	-.71
CNN	number of user to average (centralized)	< .001	-.79
	dirichlet $\alpha$	.76	.074
	unbalance sgm	.84	.049
	number of user in partition	< .001	-.83
	maximum number of classes (10 users)	.009	.45
	maximum number of classes (100 users)	.005	.67
	number of user to average (30 users)	< .001	-.77
	number of user to average (centralized)	< .001	-.83

We can see, as reported in Section 5.1 and 5.2, all experiments except the CNN experiments on dirichlet  $\alpha$  and unbalance sgm can demonstrate significant correlation under a significance level of 0.1. More to the point, we report numerous correlations with p-value less than .001 (significant under level of .001). This Hypothesis Testing validated the findings of our investigation.

## D Different aggregation method

To further validate the observation in Section 5.2 and see if this phenomenon generalizes to different aggregation methods. We perform the same experiment on three different aggregation methods, namely Krum [6], Geometric Mean [44] and Trimmed Mean [44]. As per Figure 6, we can see that with all three aggregation methods, there are decreasing trends as the number of averaged users per round increases similar as Figure 3. This further demonstrates our observations in Section 5.2 and support theoretical results in Section 6.

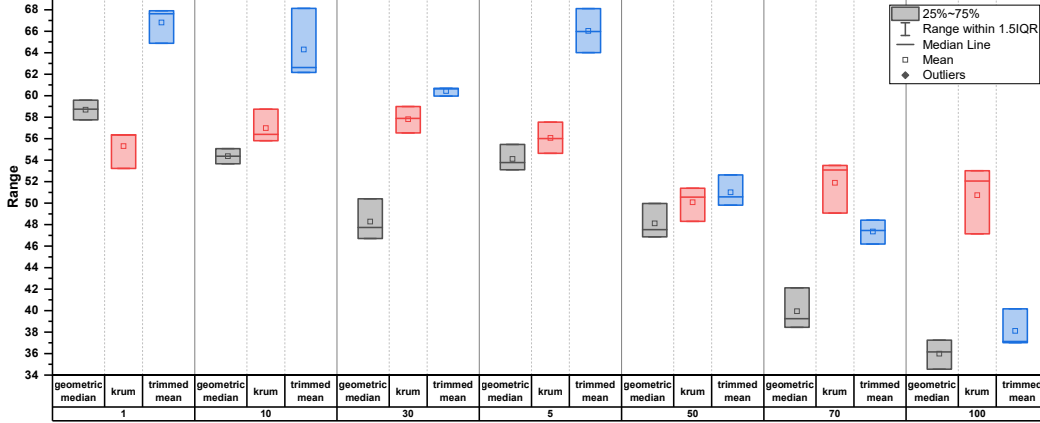


Figure 6: Transfer rate v.s. different number of clients selected to average in each round of difference aggregation method.

## E Does different partition matters in transfer attack?

In Section 4.2, we discover that with source model trained in federated manner, T.Rate can be boosted to the highest of 99%. Since we assume that the attacker have information regarding the data partition of all malicious clients, we leverage the same partition used in target model to train the source model. In this section, we are curious about whether different partitions used by source model effects the transferability of its adversarial examples against the target model. That is, whether using a partition different from the target model to train the source model affects the transfer rate of its adversarial examples. To explore such setting, we first randomly generates two different partitions with distinct random seeds and then perform the source model training and transfer attack the same as in Section 4.2. We repeat the experiment 4 times with different random seeds and report the mean results in Figure 7. We observe no significant difference between the same partition and the different partition setting. To further validate this observation, we perform Hypothesis Test on the obtained results with Paired Sample T-Test. The p-value .393 means that there is no significant difference between the transfer rate obtained by same and different partition. This investigation and result further improve the possibility of attacking a FL system through black-box attack.

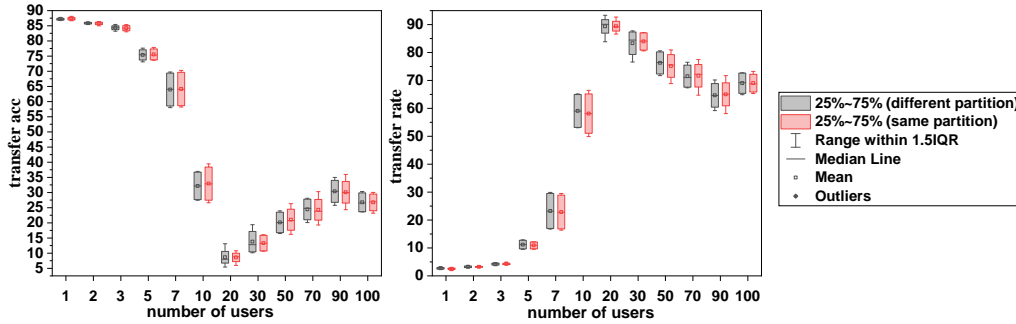


Figure 7: Difference between same partition and different partition; Left: transfer accuracy v.s. number of users' data leveraged in source model training; Right: transfer rate v.s. number of users' data leveraged in source model training;

## F Relative Increase R

For simplicity, we derive another metric for theoretical analysis. We follow [11] and define the transferability to be the loss of the target model of an adversarial example, which can be simplified



through a linear approximation of the loss function:

$$T = l(f(x + \hat{\delta}; \theta), y) \quad (12)$$

$$\approx l(f(x; \theta), y) + \hat{\delta}^T \nabla_x l(f(x; \theta), y) \quad (13)$$

where  $\hat{\delta}$  is some perturbation generated by the surrogate model, which corresponds to the maximization of an inner product over an  $\epsilon$ -sized ball under the above linear approximation:

$$\hat{\delta} \in \arg \max_{\|\delta\|_p < \epsilon} l(f'(x + \delta; \theta'), y) \quad (14)$$

$$\max_{\|\delta\|_p < \epsilon} \delta^T \nabla_x l(f'(x; \theta'), y) = \epsilon \|\nabla_x l(f'(x; \theta'), y)\|_q \quad (15)$$

where  $\|\cdot\|_q$  and  $\|\cdot\|_p$  are dual norm.

Without loss of generality, we take  $p = 2$  and gives optimal  $\hat{\delta} = \epsilon \frac{\nabla_x l(f'(x; \theta'), y)}{\|\nabla_x l(f'(x; \theta'), y)\|_2}$  from the surrogate model. Substituting it back to the Equation 13 we have the loss increment, bounded by the loss of the white-box attack:

$$\Delta l = \epsilon \frac{\nabla_x l(f'(x; \theta')^T \nabla_x l(f(x; \theta), y)}{\|\nabla_x l(f'(x; \theta'), y)^T\|_2} \leq \epsilon \|\nabla_x l(f(x; \theta), y)\|_2 \quad (16)$$

We define the relative increase in loss in black-box case compared to white box as  $R(x, y)$  which we show has a lower bound.

$$R(x, y, \theta, \theta') = \frac{\nabla_x l(f'(x; \theta'), y)^T \nabla_x l(f(x; \theta), y)}{\|\nabla_x l(f'(x; \theta'), y)\|_2 \|\nabla_x l(f(x; \theta), y)\|_2} \quad (17)$$

## G Proof of Theorem 6.2

We give the rest of assumptions for Theorem 6.2 which is taken from [26].

**Assumption 4:** The loss function  $l$  is  $L$ -smooth: for all  $v$  and  $w$ ,  $l(v) \leq l(w) + (v - w)^T \nabla l(w) + \frac{L}{2} \|v - w\|_2^2$ .

**Assumption 5:** The loss function  $l$  is  $\mu$ -strongly convex: for all  $v$  and  $w$ ,  $l(v) \geq l(w) + (v - w)^T \nabla l(w) + \frac{\mu}{2} \|v - w\|_2^2$ .

**Assumption 6:** Let  $\xi_t^k$  be sampled from the  $k$ -th device's local data uniformly at random in iteration  $t$ . The variance of stochastic gradients in each device is bounded by  $\sigma_k^2$ :  $\mathbb{E} \|\nabla l(\xi_t^k; \theta_t^k) - \nabla l(\theta_t^k)\| \leq \sigma_k^2$

**Assumption 7:** The expected squared norm of stochastic gradients is uniformly bounded, i.e.,  $\mathbb{E} \|\nabla l(\xi_t^k; \theta_t^k)\|^2 \leq G^2$  for all  $k = 1, \dots, N$  and  $t = 1, \dots, T - 1$ .

**Assumption 8:** We assume the federated algorithm is FedAvg. Assume  $S_t$  contains a subset of  $K$  indices randomly selected with replacement according to the sampling probabilities  $p_1, \dots, p_N$ . The aggregation step of FedAvg performs  $\theta_t \leftarrow \frac{1}{K} \sum_{k \in S_t} \theta_t^k$ .  $\theta_t^k$  denotes the parameters of device  $k$  at iteration  $t$ .

We use Theorem 2 from [26] as our lemma to prove our Theorem 6.2.

**Lemma G.1.** *With assumption 4 to 8 and  $L, \mu, \sigma_k$  and  $G$  be defined therein. Let  $L^*$  denote the minimum loss obtained by optimal estimation from the centralized model and  $l(\theta')$  denotes the loss of the federated model. Then*

$$\mathbb{E}[l(\theta')] - L^* \leq \frac{\kappa}{\gamma + T - 1} \left( \frac{2(B + C)}{\mu} + \frac{\mu\gamma}{2} \mathbb{E} \|\theta_1 - \theta_\star\| \right) \quad (18)$$

where  $L, \mu, \sigma_k, G$  is defined in the assumptions,  $\kappa = \frac{L}{\mu}$ ,  $\gamma = \max\{8\kappa, E\}$ ,  $B = \sum_{k=1}^N p_k^2 \sigma_k^2 + 6L\Gamma + 8(E - 1)^2 G^2$  and  $C = \frac{4}{K} E^2 G^2$ .  $\theta_1$  is the parameter after one step update of SGD.  $\theta_\star$  is the optimal parameter for centralized model.

Now, we prove Theorem 6.2.

*Proof.* We first write out

$$l(\theta') - L^* = \theta'^T X^T X \theta' - \theta_*^T X^T X \theta_* \quad (19)$$

$$= (\theta' - \theta_*)^T X^T X (\theta' - \theta_*) \quad (20)$$

$$\geq \|\theta'\|_2 \|\theta_*\|_2 \quad (21)$$

when  $X^T X$  is p.s.d.

On the other hand, we can write  $l(\theta') = L^* + \epsilon$  where  $\epsilon > 0$ . Due to the construction of our model, we can write

$$\theta' = (X^T X)^{-1} X^T \sqrt{(X \theta_*)^2 + \epsilon} \quad (22)$$

by solving a linear system. Thus, we can get

$$\theta_*^T \theta' = \theta_*^T (X^T X)^{-1} X^T \sqrt{(X \theta_*)^2 + \epsilon} \quad (23)$$

$$\geq \theta_*^T (X^T X)^{-1} X^T X \theta_* \quad (24)$$

$$= \theta_*^T \theta_* \quad (25)$$

Thus, by connecting the above terms, we will have

$$R(x, y, \theta_*, \theta') = \frac{\theta'^T \theta_*}{\|\theta'\|_2 \|\theta_*\|_2} \geq \frac{\theta_*^T \theta_*}{l(\theta') - L^*} \quad (26)$$

Finally, by substituting Equation 18 to the denominator, we have

$$\mathbb{E}[R(x, y, \theta', \theta_*)] \geq \frac{(\gamma + T - 1) \theta_*^T \theta_*}{\kappa \left( \frac{2(B+C)}{\mu} + \frac{\mu\gamma}{2} \mathbb{E}\|\theta_1 - \theta_*\|^2 \right)} \quad (27)$$

$$= \frac{2\mu(\gamma + T - 1) \theta_*^T \theta_*}{4(B+C)\kappa + \mu^2 \gamma \kappa \mathbb{E}\|\theta_1 - \theta_*\|^2} \quad (28)$$

□

## H Proof of Theorem 6.6

*Proof.* We adopt the Bias-Variance decomposition [16] to provide theoretical justification for the observation in Section 5.2. Let  $\mathcal{T}$  denote the train set  $\mathcal{T} = (X, Y)$  sampled from some data distribution and  $x'$  denote the adversarial example following some adversarial distribution. First, we give the Bias-Variance decomposition as follows:

$$\mathbb{E}_{x', y} \mathbb{E}_{\mathcal{T}} [\|y - f(x'; \mathcal{T})\|_2^2] = \underbrace{\mathbb{E}_{x', y} [\|y - \bar{f}(x')\|_2^2]}_{\text{Bias}^2} + \underbrace{\mathbb{E}_{x', \mathcal{T}} [\|\bar{f}(x') - f(x'; \mathcal{T})\|_2^2]}_{\text{Variance}} \quad (29)$$

where  $f(\cdot; \mathcal{T})$  denotes a model  $f$  trained on dataset  $\mathcal{T}$ .  $\bar{f}(\cdot) = \mathbb{E}_{\mathcal{T}} [f(\cdot; \mathcal{T})]$  is the expected model over the data distribution of  $\mathcal{T}$ . By using an average of multiple model  $f(\cdot; \mathcal{T})$ , denoted by  $f_n = \frac{1}{n} \sum_{i=1}^n f_i(\cdot; \mathcal{T}_i)$  and with  $\bar{f}_n(\cdot) = \mathbb{E}_{\mathcal{T}} [\frac{1}{n} \sum_{i=1}^n f_i(\cdot; \mathcal{T}_i)] = \bar{f}(\cdot)$ , we can show the following:

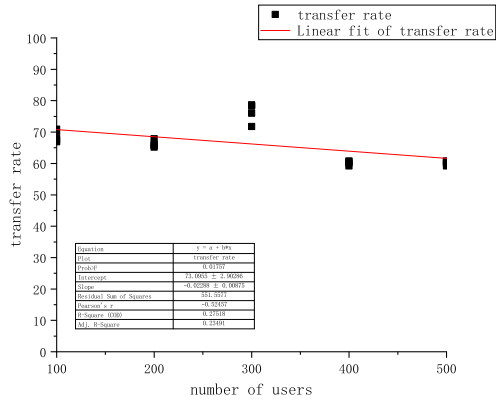
$$\mathbb{E}_{x', y} \mathbb{E}_{\mathcal{T}} [\|y - f_n(x')\|_2^2] = \underbrace{\mathbb{E}_{x', y} [\|y - \bar{f}_n(x')\|_2^2]}_{\text{Bias}^2} + \underbrace{\mathbb{E}_{x', \mathcal{T}} [\|\bar{f}_n(x') - f_n(x')\|_2^2]}_{\text{Variance}} \quad (30)$$

$$= \mathbb{E}_{x', y} [\|y - \bar{f}(x')\|_2^2] + \frac{1}{n} \mathbb{E}_{x', \mathcal{T}} [\|\bar{f}(x') - f(x', \mathcal{T})\|_2^2] \quad (31)$$

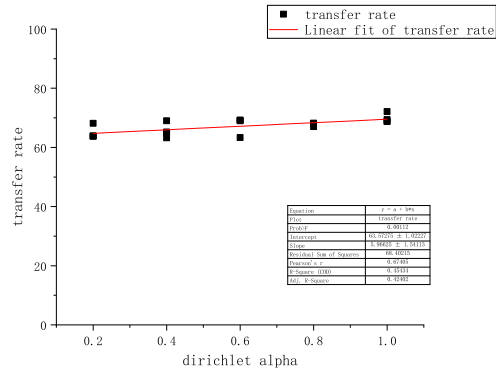
Inequality 11 holds due to that  $\text{Var}(\frac{1}{n} \sum_{i=1}^n f_i(\cdot; \mathcal{T}_i)) = \frac{1}{n^2} \text{Var}(\sum_{i=1}^n f_i(\cdot; \mathcal{T}_i))$  and since each  $f_i$  is trained independently,  $\frac{1}{n^2} \text{Var}(\sum_{i=1}^n f_i(\cdot; \mathcal{T}_i)) = \frac{1}{n^2} \sum_{i=1}^n \text{Var}(f_i(\cdot; \mathcal{T}_i)) = \frac{1}{n} \text{Var}(f(\cdot; \mathcal{T}))$ . □

## I linear regression to visualize the correlation

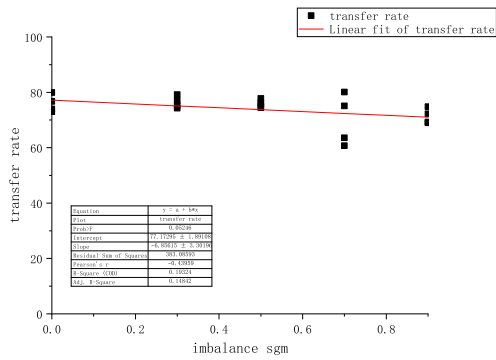
To better demonstrates the correlation between various factors and adversarial transferability, we perform linear regression with hypothesis testing on the experiment results. We plot scatter graph and linear regression line on each of the correlation and corresponding experiment result as shown in the following figures:



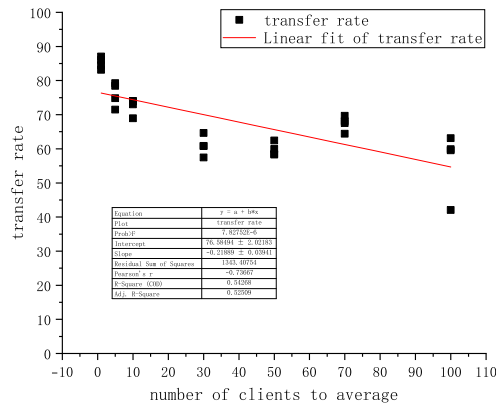
(a) ResNet50: transfer rate v.s. number of total users in the partition.



(b) ResNet50: transfer rate v.s. dirichlet alpha.

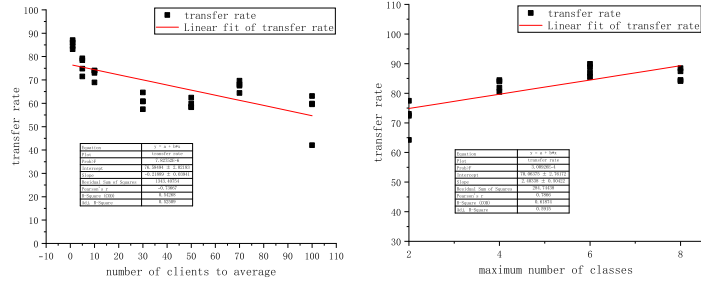


(c) ResNet50: transfer rate v.s. unbalance sgm.

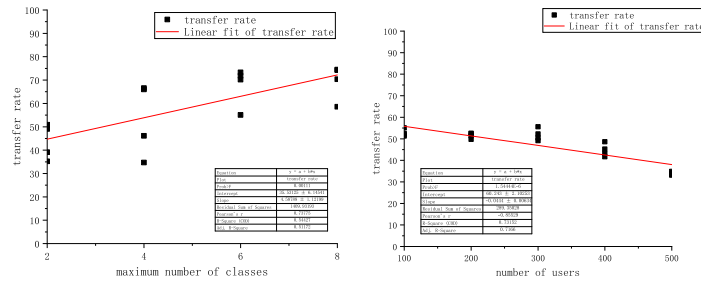


(d) ResNet50: transfer rate v.s. number of users to average per round (source model trained in centralized manner with full training dataset).

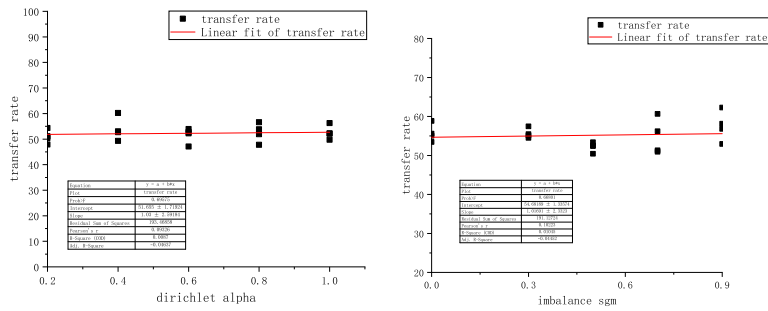
Figure 8: Linear regression visualization



(a) ResNet50: transfer rate v.s. num- (b) ResNet50: transfer rate v.s. maxi-  
 number of users to average per round mum number of classes per user (10  
 (source model trained in centralized users)..  
 manner with 30 client's data).

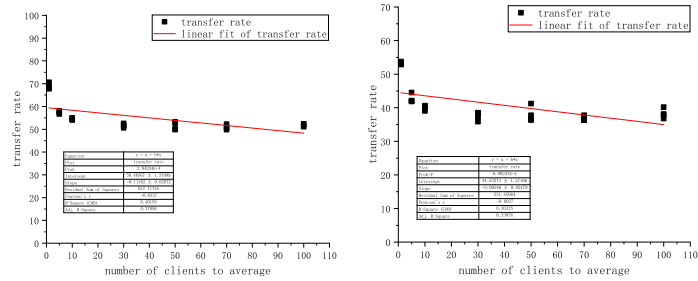


(c) ResNet50: transfer rate v.s. the (d) CNN: transfer rate v.s. the number  
 maximum number of classes per user of total users in the partition.  
 (100 users).

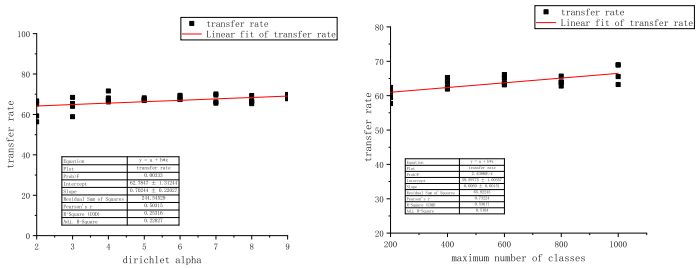


(e) CNN: transfer rate v.s. dirichlet alpha. (f) CNN: transfer rate v.s. unbalance sgm.

Figure 9: Linear regression visualization



(a) CNN: transfer rate v.s. number of users to average per round (source model trained in centralized manner with full training dataset). (b) CNN: transfer rate v.s. number of users to average per round (source model trained in centralized manner with 30 client's data).



(c) CNN: transfer rate v.s. maximum number of classes per user (10 users). (d) CNN: transfer rate v.s. the maximum number of classes per user (100 users).

Figure 10: Linear regression visualization